Polymer 53 (2012) 939–946

Contents lists available at SciVerse ScienceDirect

Polymer

journal homepage: www.elsevier.com/locate/polymer

# Quenching effects of gold nanoparticles in nanocomposites formed in water-soluble conjugated polymer nanoreactors

Po-Jen Yang [a], Hsuan-Chih Chu [a], Yu-Hsien Lee [b], Takayoshi Kobayashi [b], Te-Cheng Chen [a], Hong-Cheu Lin [a,*]

[a] Department of Materials Science and Engineering, National Chiao Tung University, Taiwan, ROC
[b] Department of Electrophysics, National Chiao Tung University, Hsinchu, Taiwan, ROC

ARTICLE INFO

*Article history:*
Received 6 October 2011
Received in revised form
22 December 2011
Accepted 25 December 2011
Available online 3 January 2012

*Keywords:*
Gold nanoparticle
Water-soluble conjugated polyfluorene
Aqueous surfactant

ABSTRACT

In this paper we describe the first example of the in situ synthesis of gold nanoparticles (**AuNPs**) in the presence of a water-soluble conjugated polyfluorene (**NPF**) presenting pendent ammonium groups, with the polymer acting as an aqueous surfactant and providing fluorescent nanoreactors. Using this approach, we produced well-dispersed **NPF-AuNP** nanocomposites without the need for any additional reducing agents. The photoluminescence emission intensity of **NPF-AuNP** nanocomposite solution was quenched to a greater extent upon increasing the concentration of **AuNPs**, presumably through energy transfer or electron transfer from the fluorescent polymer to the metal nanoparticles. Through variations in the degrees of protonation and deprotonation of the amino groups of **NPF** at different values of pH, we found that the extent of quenching of **AuNPs** in **NPF-AuNP** nanocomposite solutions was directly related to the adsorption and desorption behavior of **NPF** on the metal surfaces. Transmission electron microscopy revealed that the greatest aggregation of **AuNPs** in the nanocomposite solution occurred at pH 3, suggesting that the ammonium groups ($RNMe_2$ at pH 8.5; $RNMe_2H^+$ at pH 3) of the polymer side chains adsorbed onto the **AuNP** surfaces under these conditions. Distinct time-resolved fluorescence signals of the **AuNP**-quenched **NPF** polymers at different values of pH confirmed the interactions between these species.



## 1. Introduction

Several methods are available for the preparation of polymers as functional surfactants that interact with metal structures, with applications in the development of biological, optical, and pH sensors [1–5]. Because gold structures on the nanometer size scale exhibit widely size-dependent electronic, chemical, and optical properties [6–8], the surface functionalization of gold nanoparticles (**AuNPs**) of various sizes has been exploited for a number of applications. **AuNPs** are commonly synthesized in the aqueous phase through the chemical reduction of chloroaurate precursors (typically chloroauric acid, $HAuCl_4$) mediated by sodium citrate, with stabilizers presenting ionic or acidic functional groups often used as surfactants to generate **AuNPs** with certain characteristic properties [9,10]. Nanocomposites fabricated from polymers and **AuNPs** have several potential biological applications because of their nontoxicity, biocompatibility, ease of imaging, and the versatile surface chemistry of **AuNPs** [11,12]. In particular, water-soluble (non-conjugated) polymers containing amino groups can be used as stabilizing and capping agents for **AuNPs** during the reduction of chloroaurate precursors in aqueous solutions [13,14].

It is well established that metallic surfaces induce strong quenching of molecular fluorescence as a result of energy transfer or electron transfer from the fluorescent molecules to the metals [15,16]. The quenching of the fluorescence of conjugated polymers by **AuNPs** has been used recently to develop novel fluorescent biosensors for the detection of DNA and for other bio-related applications in aqueous media [17–20]. Moreover, modifications of **AuNPs** and the polymeric fluorophores are essential for the development of biological labels as well as for optoelectronic applications that take advantage of the strong quenching effects induced by the large total surface areas of the nanoparticles. In chromophore/**AuNP** nanocomposites, the molecular excitation energy of the chromophores can be transferred efficiently to **AuNPs**, thereby quenching the emission [21,22]. Several theoretical models of fluorescent nanocomposites have been developed recently to predict the effects of various parameters (e.g., the sizes of **AuNPs**; the distance between the chromophore and **AuNP** units) on the fluorescence quenching phenomena [23–27]. The assembly

* Corresponding author. Tel.: +886 3 5712121x55305; fax: +886 3 5724727.
*E-mail addresses:* linhc@mail.nctu.edu.tw, linhc@cc.nctu.edu.tw (H.-C. Lin).

0032-3861/$ – see front matter © 2012 Elsevier Ltd. All rights reserved.
doi:10.1016/j.polymer.2011.12.049

of water-soluble conjugated polymer/**AuNPs** composites, in particular, may provide a route to potential biological applications of **AuNPs** through improved mechanical, optical, and delivery properties [28–31]. For further bio-developments of nanocomposites, it would be preferable to ensure that the metal nanoparticles and fluorescent conjugated polymers were well dispersed in the aqueous solutions. Herein, we report a facile method for the in situ synthesis of **AuNPs** in an aqueous solution of a conjugated polyfluorene (**NPF**) presenting dimethylammonium side chains, where **AuNPs** were encapsulated within the water-soluble **NPF**, which acted as a surfactant and also behaved as a water-soluble conjugated polymer nanoreactor. Fig. 1 illustrates the formation of the nanocomposites **NPF-AuNPs** through reduction of an aqueous solution of chloroauric acid in the presence of the polymer surfactant **NPF**. Ammonium ions are often used to bind and reduce chloroauric ($AuCl_4^-$) ions and stabilize the resulting **AuNPs** as a result of their high affinities to metallic gold [32,33]. Therefore, polymers containing amino groups (as binding sites) have been used broadly to interact with anionic gold complex ions and as capping agents to control nanoparticle growth [34–36]. The interactions between conjugated polymers and **AuNPs** in aqueous solutions at different values of pH can lead to different quenching effects in the fluorescent nanocomposites, due to the different degrees of protonation and deprotonation of the amino groups in the gold colloids [37]. The protonation of amino groups of polymers at low pH will lead to the ammonium ions adsorbing on the gold surfaces, resulting in aggregation of **AuNPs** and, thereby, quench of any fluorescence emission (e.g., for **NPF**). Fluorescent nanocomposites containing water-soluble conjugated polymers and **AuNPs** might have practical use in the development of chemosensors or biosensor applications.

## 2. Experimental

### 2.1. Materials

All chemicals were purchased from Aldrich and Sigma–Aldrich and used without further purification. Ultrapure filtered water (resistivity: 18.2 MΩ) was used in all experiments. The water-soluble conjugated polymer was synthesized through Suzuki coupling according to pervious reports [38,39]. The synthetic procedure for the preparation of water-soluble conjugated polyfluorene **NPF** is presented in Scheme 1.

### 2.2. Synthesis of monomers and polymers

#### 2.2.1. 2,7-Dibromo-9,9-bis(6′-bromohexyl)fluorene (*1*)

2,7-Dibromofluorene (1 mmol) was added to a mixture of 50 wt % aqueous NaOH (50 mL), tetrabutylammonium bromide (1 mmol), and 1,6-dibromohexane (10 mmol) at 75 °C. After 4 h, the mixture was cooled to room temperature and extracted with $CH_2Cl_2$. The combined organic extracts were washed successively with water, 0.5 M HCl, water, and brine and then dried ($MgSO_4$). The solvent was evaporated under reduced pressure and the excess 1,6-dibromohexane was removed through vacuum distillation; the residue was purified chromatographically ($SiO_2$; hexane/$CH_2Cl_2$, 10:1) to yield a white solid (59%). $^1$H MNR ($CDCl_3$, ppm), $\delta$: 7.41–7.52 (m, 6H), 3.28–3.33 (t, 4H), 1.92–1.97 (m, 4H), 1.61–1.71 (m, 4H), 1.03–1.26 (m, 8H), 0.53–0.65 (m, 4H).

#### 2.2.2. 2,7-Dibromo-9,9-bis(6′-(N,N-dimethylamino)hexyl)fluorene (*2*)

40 wt% Aqueous dimethylamine (20 mmol, 2 mL) was added dropwise under $N_2$ to a stirred solution of compound **1** in THF (50 mL) over 1 h at 0 °C and then the mixture was heated under reflux overnight. The reaction mixture was poured into cold water and extracted with $CH_2Cl_2$; the extracts were dried ($MgSO_4$) and concentrated under vacuum at 45 °C. The residue was purified by chromatographically ($SiO_2$; hexane/EtOAc, 5:1) to yield a light-yellow solid (76%). $^1$H NMR ($CDCl_3$, ppm), $\delta$: 7.47–7.57 (m, 6H), 3.30–3.37 (m, 4H), 2.98 (s, 12H), 1.94–2.20 (m, 4H), 1.63–1.74 (m, 4H), 1.07–1.30 (m, 8H), 0.54–0.69 (m, 4H). Anal. Calcd for [$C_{29}H_{42}Br_2N_2$]: C, 60.21; H, 7.32; N, 4.86; found: C, 60.19; H, 9.14; N, 7.37.

#### 2.2.3. Poly{9,9-bis[6′-(N,N-dimethylamino)hexyl]fluorene-co-alt-1,4-phenylene} (*3*)

Compound **2** (10 mmol) and 1,4-benzenediboronic acid bispinacol ester (10 mmol) were dissolved in THF (10 mL) in a 50-mL

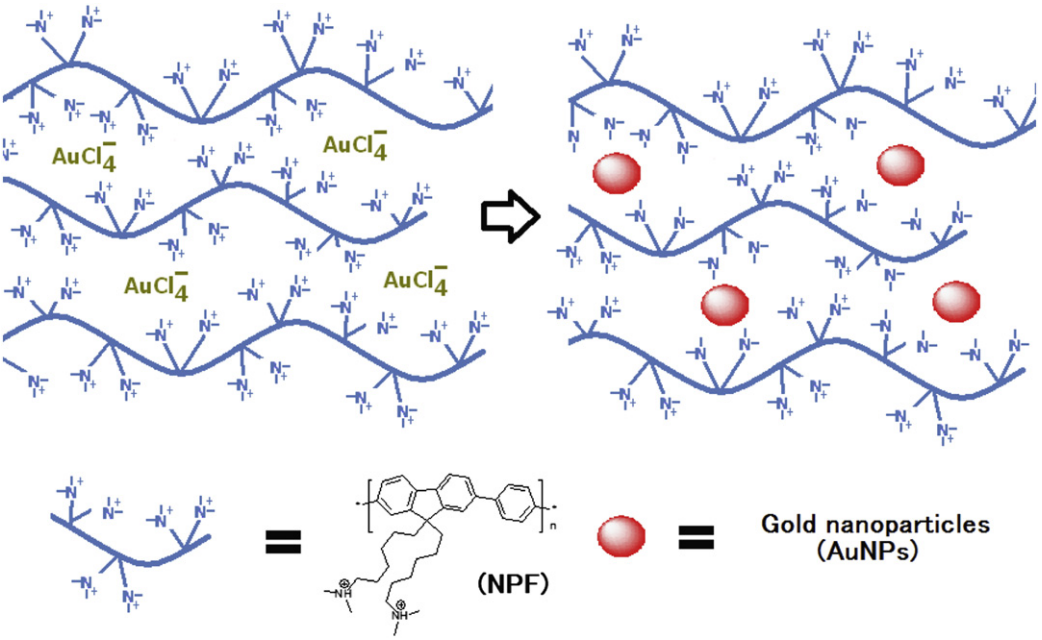


**Fig. 1.** Formation of **NPF-AuNP** nanocomposites through reduction of $AuCl_4^-$ ions in an aqueous solution of polymer **NPF** (acting as a water-soluble conjugated polymer nanoreactor).

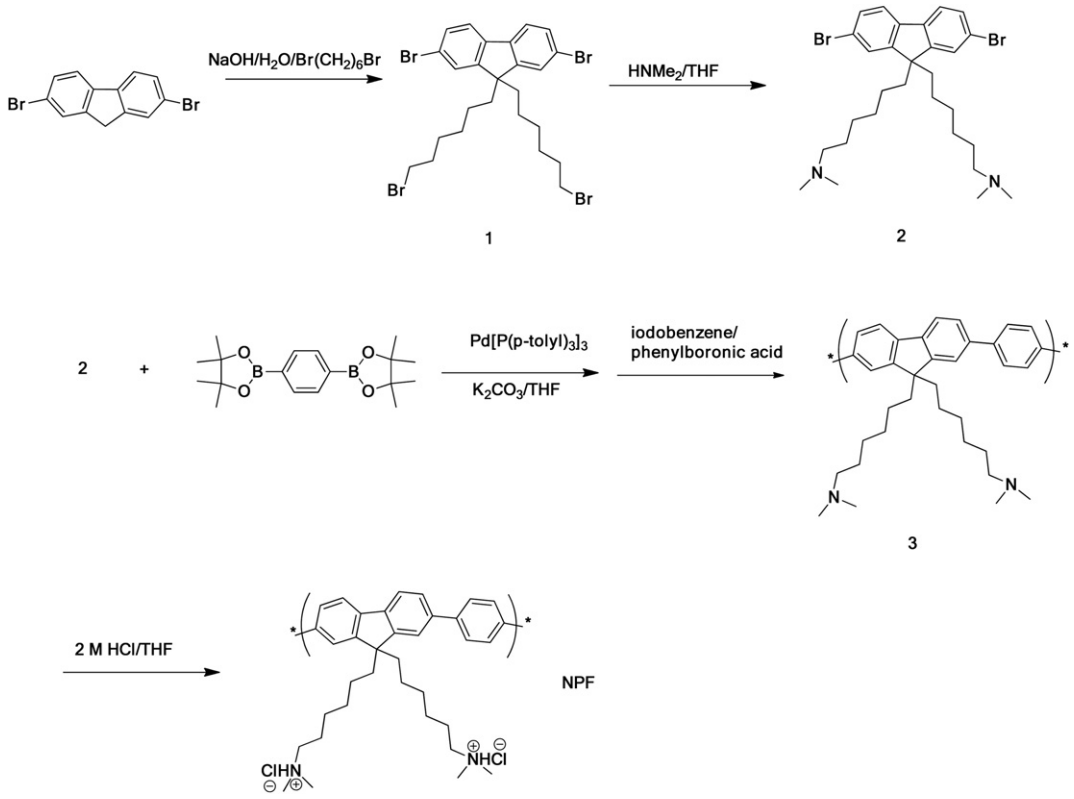


**Scheme 1.** Synthesis of Polymer NPF.

two-neck flask. Pd[P(*p*-tolyl)$_3$]$_3$ (1 mol % of total monomer concentration) was washed with acetone, dried, and transferred into the flask. 2 M Aqueous $K_2CO_3$ and the phase transfer catalyst Aliquat 336 (several drops) were subsequently transferred via cannula into the solution under $N_2$. The reaction mixture was stirred at 75 °C for 3 days and then excess amounts of iodobenzene and phenylboronic acid (end-cappers) dissolved in THF (1 mL) were added individually and stirred for 4 h, respectively. The reaction mixture was cooled to 50 °C and added slowly into a vigorously stirred mixture of MeOH (300 mL) and water (100 mL). The pre-polymer (compound **3**) was collected by filtration and reprecipitated from MeOH. Yield: 71%. $^1$H MNR (DMSO-$d_6$, ppm), $\delta$: 8.06–7.96 (br, m, 4H), 7.91–7.79 (br, m, 6H), 3.15–3.12 (br, m, 4H), 2.91–2.80 (br, m, 12H), 2.56–2.53 (br, m, 4H), 1.03 (br, m, 16H).

#### 2.2.4. Poly{9,9-bis[6′-(N,N-dimethylammonium)hexyl]fluorene-co-alt-1,4-phenylene} dichloride (*NPF*)

The pre-polymer **3** (0.1 mmol) and 2 M HCl (10 mL) were dissolved in THF (5 mL) at room temperature. After 24 h, diethyl ether was added and the mixture was extracted with water. The aqueous phase was concentrated and the residual **NPF** was precipitated from EtOH. Yield: 59%. $^1$H MNR (DMSO-$d_6$, ppm), $\delta$: 8.08–7.99 (br, m, 4H), 7.87 (br, m, 4H), 7.72 (br, m, 2H), 3.15 (br, m, 4H), 2.93–2.86 (br, m, 12H), 2.59–2.55 (br, m, 4H), 1.05 (br, m, 16H). Number-average molecular weight ($M_n$): 32,000 g/mol; polydispersity index (PDI): 1.2 (determined using GPC). Decomposition temperature ($T_d$): 280 °C (determined by 5% weight loss in TGA). Glass transition temperatures ($T_g$) could not be obtained by DSC.

### 2.3. Growth of AuNPs in aqueous solution

An **NPF** stock solution (prepared in water at concentrations from 0 to $5 \times 10^{-2}$ mM) was added to $HAuCl_4$ solution (2 mM) and then the pH of the solution was adjusted to pH 8.5 by adding 0.1 M NaOH (a few microliters). The solution was placed in a water bath (45 °C) for 4 h, resulting in a solution having a color in the range from light yellow to pink. Transmission electron microscopy (TEM) and UV–vis absorption spectra were used to characterize the shapes and sizes of the nanoparticles. The suspensions of the gold nanoparticles (**AuNPs**) in the nanocomposite solutions were subsequently adjusted to various values of pH to study the quenching behavior of the nanoparticles. The fluorescence of the nanocomposite (**NPF-AuNPs**) solutions was quenched to different degrees when different concentrations of the gold precursor were used.

### 2.4. Measurements and characterization

$^1$H NMR spectra were recorded using a Varian Unity 300 $MH_Z$ spectrometer and $CDCl_3$ solutions. Elemental analyses were performed using a HERAEUS CHN-OS RAPID elemental analyzer. Gel permeation chromatography (GPC) was conducted using a Waters 1515 separation module with polystyrene as the standard and DMF as the eluent. Transition temperatures were determined by differential scanning calorimetry (DSC, model: Perkin–Elmer Diamond) under $N_2$ with a heating and cooling rate of 10 °C/min. Thermogravimetric analyses (TGA) were carried out on a TA Instruments Q500 thermogravimetric analyzer at a heating rate of 20 °C/min under nitrogen. UV–vis absorption spectra of water solutions were recorded using a Jasco V-670 spectrophotometer; photoluminescence (PL) spectra were recorded using a Hitachi F-4500 spectrophotometer. Both types of spectra were recorded from samples in a quartz cell (optical path: 10 mm). PL spectra were measured at the excitonic emission (ca. 379 nm). The PL quenching behavior followed the Stern–Volmer relation

$$I_0/I = 1 + K_{SV}[Q]$$

where $I_0$ and $I$ are the PL emission intensities of the water-soluble fluorescent conjugated polymer **NPF** in the absence and presence of the quencher Q (**AuNPs**), respectively; $K_{SV}$ is the Stern–Volmer quenching constant [40]; and [Q] is the concentration of the quencher.

Transmission election microscopy (TEM) was performed using a JEOL 2100 electron microscope operated at an acceleration voltage of 200 keV. The samples prepared from aqueous solutions were collected on Cu TEM grids (200 mesh/carbon films) and left to dry completely. Time-resolved photoluminescence (TRP) spectra were measured using a home-built single-photon-counting system. Excitations were performed using a 375-nm diode laser (Picoquant PDL-200, 50 ps fwhm, 2 M Hz). The signals collected at the excitonic emissions of solutions ($\lambda$ = 421 nm) were connected to a time-correlated single-photon-counting card (TCSPC, Picoquant Timeharp 200). The emission decay data were analyzed with biexponential kinetics, from which two decay components were derived; the values of the lifetimes ($\tau_1$ and $\tau_2$) and pre-exponential factors ($A_1$ and $A_2$) of **NPF** in the nanocomposite (**NPF-AuNPs**) solutions were determined.

## 3. Results and discussion

### 3.1. Reduction of $HAuCl_4$ in the presence of *NPF*

The water-soluble conjugated polymer **NPF** was synthesized through Suzuki coupling using procedures described in the literature [34,35]. **NPF** was used to reduce $HAuCl_4$ into **AuNPs** and also as a conjugated polyelectrolyte for fluorescence resonance energy transfer (FRET). The maximum absorption and emission bands of **NPF** appeared at 379 and 421 nm, respectively (in aqueous solutions). As demonstrated previously [39,41], the presence of ammonium ions on the side chains of **NPF** provided environments for the formation of **AuNPs**, with the polymer behaving as both a water-soluble surfactant and a reductant for $HAuCl_4$. Fig. 1 presents a possible mechanism for the formation of the nanocomposites **NPF-AuNPs** through the reduction of $HAuCl_4$ in an aqueous solution of **NPF** (behaving as a water-soluble conjugated polymer nanoreactor), which contains a conjugated fluorene backbone and hydrophilic ammonium ions on the side chains. Under these processing conditions, the ammonium groups of **NPF** were bound electrostatically to the oppositely charged gold precursor ions ($AuCl_4^-$). The polymer-bound $AuCl_4^-$ ions were slowly reduced into **AuNPs** under the weakly basic conditions of the aqueous polymer solutions. Signals corresponding to the surface plasmon resonance (SPR) absorption band at 532 nm confirmed the formation of **AuNPs**. The intensity and wavelength of the maximum absorption ($\lambda_{max}$) SPR bands are known to be correlated with the size and concentration of gold nanoparticles [37]. The presence of different amounts of **NPF** (from 0 to $5 \times 10^{-2}$ mM) in the aqueous $HAuCl_4$ solutions resulted in a color change from light yellow (initially) to typical red (finally) after stirring for 4 h, indicating that the side chains of **NPF** had reduced the $AuCl_4^-$ ions to form **AuNPs**. The UV–vis absorption spectra of the aqueous nanocomposite (**NPF-AuNPs**) solutions [Fig. 2(a)] featured two maximum absorption bands at 379 and 532 nm, which are characteristic peaks of

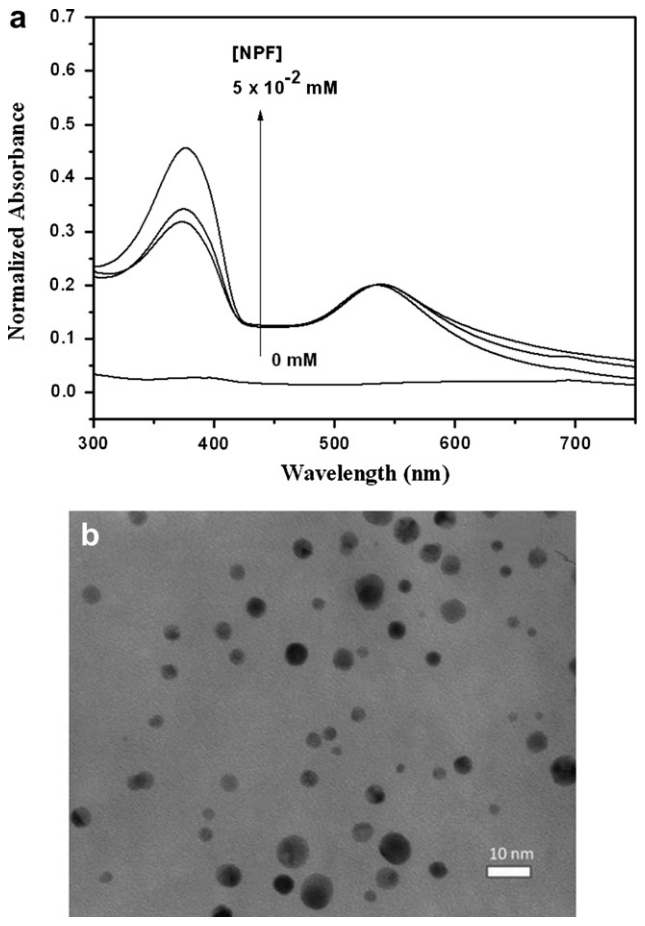


**Fig. 2.** (a) The normalized UV–vis absorption spectra of various **NPF-AuNP** nanocomposites after in situ reduction of aqueous solutions of $HAuCl_4$ ($[AuCl_4^-] = 2$ mM) in the presence of **NPF** at concentrations of 0, $1.25 \times 10^{-2}$, $2.5 \times 10^{-2}$, and $5 \times 10^{-2}$ mM (b) TEM image of **NPF-AuNP** nanocomposite containing **AuNPs** reduced from 2 mM $AuCl_4^-$ in an aqueous solution of **NPF** ($5 \times 10^{-2}$ mM).

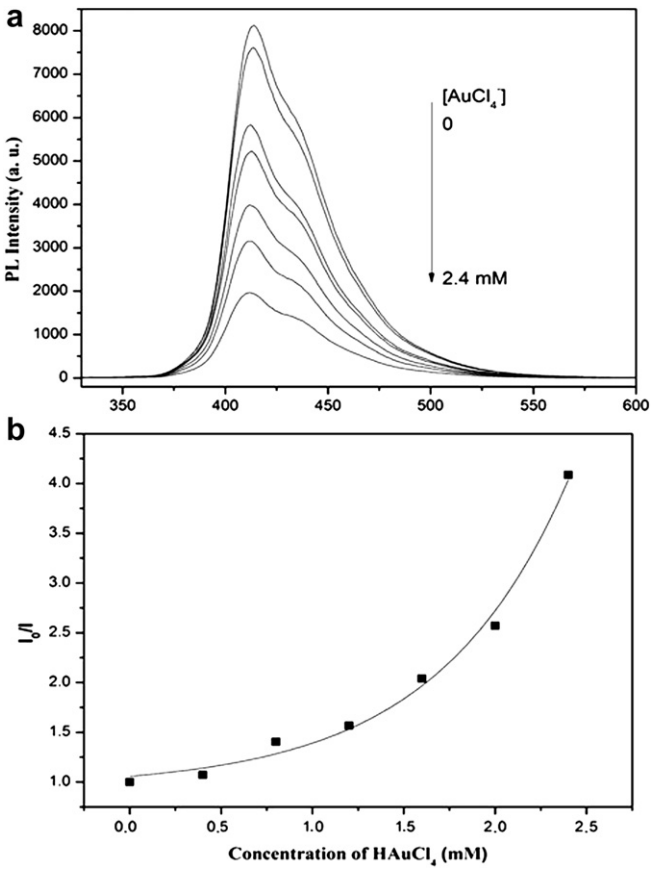


**Fig. 3.** (a) Fluorescence quenching spectra and (b) Stern–Volmer plots of polymer **NPF** in **NPF-AuNP** nanocomposites after complete growth (4 h) of **AuNPs** in aqueous solutions of $HAuCl_4$ at concentrations from 0 mM to 2.4 mM.

**NPF** and **AuNPs**, respectively. Fig. 2(a) reveals that more $AuCl_4^-$ ions were reduced in the nanocomposite solution upon increasing the concentration of **NPF** from 0 to $5 \times 10^{-2}$ mM, as indicated by the enhanced intensity of the SPR absorption band of (**AuNPs** at 532 nm absorption), which also indicated the average sizes of **AuNPs**. Fig. 2(b) displays the sizes and shapes of **AuNPs** as examined using TEM; the nanoparticles in **NPF-AuNP** nanocomposite derived from 2 mM $AuCl_4^-$ in an aqueous solution of **NPF** ($5 \times 10^{-2}$ mM) exhibited spherical morphologies with particle diameters ranging from 2 to 8 nm (average diameter: 4.5 nm).

### 3.2. Fluorescence of *NPF* in the presence of *AuNPs*

Metallic surfaces induce strong quenching of molecular fluorescence as a result of electromagnetic coupling between the metal and the fluorescent molecules; in particular, nanoparticle-induced fluorescence quenching has been studied widely [42–44]. When fluorescent polymers are used as probes for the surface plasmon fields in the vicinity of **AuNPs**, the fluorescence intensity of the polymers in direct contact with the gold nanostructures is a function of the distance between the probe polymer chains and the metal surfaces [45]. Because the PL emission of our fluorescent conjugated polymer **NPF** could be quenched by **AuNPs**, we suspected that the PL emission intensity of **NPF-AuNP** nanocomposite in solution would decrease upon increasing the concentration of **AuNPs**. As revealed in Fig. 3(a), the PL emission intensity at 421 nm of the conjugated polymer **NPF** in the nanocomposite solution decreased upon increasing the concentration of $AuCl_4^-$ ions (from 0 to 2.4 mM), which was proportional to the concentration of **AuNPs** formed in situ. Thus, the quenching efficiency of **AuNPs** in

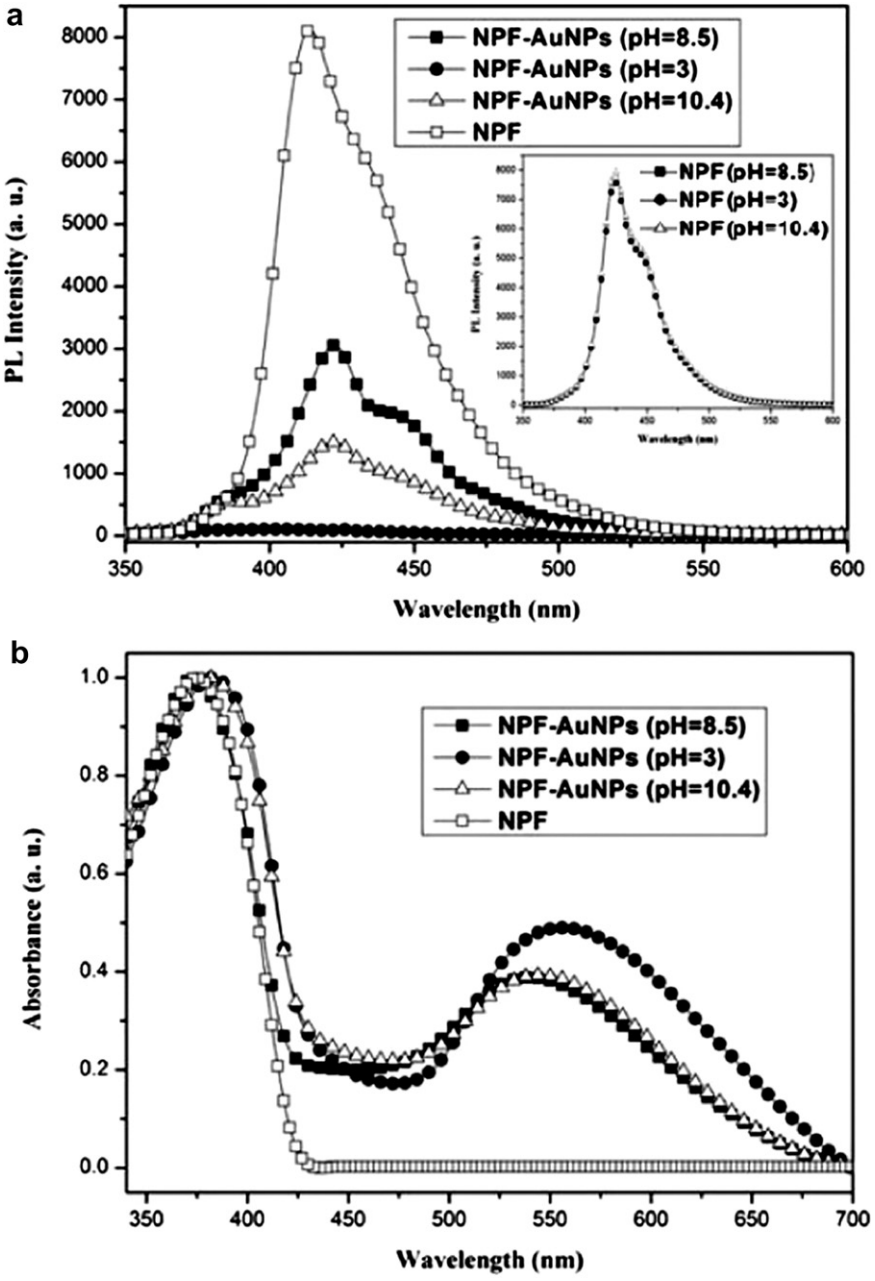


**Fig. 4.** (a) PL spectra (excited at the maximum absorption of 379 nm) and (b) UV–vis spectra of aqueous solutions of **NPF** and its **NPF-AuNP** nanocomposites at various values of pH. Inset: PL spectra of **NPF** in different pH conditions.

**NPF-AuNP** nanocomposite solution varied according to the concentration of $HAuCl_4$. Fig. 3(b) presents the Stern–Volmer plots of **NPF** in **NPF-AuNP** nanocomposites after complete growth of **AuNPs** in different concentrations of $HAuCl_4$ (from 0 to 2.4 mM), revealing that the fluorescence of **NPF** quenched by **AuNPs** in **NPF-AuNP** nanocomposite solution had a quenching constant of $4.3 \times 10^2\ M^{-1}$ (calculated from the linear region at concentrations from 0 mM to 1.4 mM). Therefore, the quantity of **AuNPs** played an important role in the fluorescence quenching of **NPF-AuNP** nanocomposite solutions.

### 3.3. pH-Dependent PL properties of *NPF-AuNP* nanocomposites

As described in the Experimental section, the color of **NPF-AuNP** nanocomposite solution changed from light yellow to red when the pH was set at pH 8.5, indicating the formation of **AuNPs** under weakly basic conditions. Subsequently, we adjusted the pH of **NPF-AuNP** solution to pH 3 by adding 0.1 M HCl and then to pH 10.4 by adding 0.1 M NaOH. We then subjected the three **NPF-AuNP** solutions (at pH 3, 8.5, and 10.4) to analyses using UV–vis and fluorescence spectroscopy, TRP, and TEM. Fig. 4(a) and (b) displays the PL (excited at the maximum absorption of 379 nm) and UV–vis absorption spectra, respectively, of the three **NPF-AuNP** solutions. The maximum PL emission of each aqueous solution in Fig. 4(a) appeared near 420 nm. The inset to Fig. 4(a) reveals that the PL intensities of **NPF** in the absence of **AuNPs** were not affected by the pH. Upon changing the pH, the fluorescence intensities of **NPF-AuNP** nanocomposite solutions decreased to different extents, with the largest PL quenching observed at pH 3, presumably because the amino groups on the polymer side chains were highly protonated under these conditions and, therefore, were adsorbed to a greater extent on the **AuNP** surfaces. The shoulder of PL at ca. 430–460 nm (pH 8.5) reflects the aggregation of polymer chains. At pH 10.4, the amino groups on the polymer side chains were neutralized considerably, leading to lower degrees of adsorption and quenching on the **AuNP** surfaces.

The UV–vis absorption spectra in Fig. 4(b) reveal the sizes of the dispersed **AuNPs** under the three values of pH, suggesting their degrees of aggregation. The SPR absorption band of **NPF-AuNPs** at pH 8.5 appeared near 532 nm. This band for **NPF-AuNP** solution at pH 3 was red-shifted to 556 nm, due to the greater size of the aggregated **AuNPs** upon protonation of the amino groups of the polymer. At pH 10.4, the SPR band of **NPF-AuNP** solution shifted back to 534 nm, due to the lower degree of aggregation of **AuNPs**. In addition, **AuNPs** in the initial **NPF-AuNP** solution at pH 8.5 possessed a spherical morphology with an approximate particle diameter of 4.5 nm [Fig. 2(b)]; greater aggregation of **AuNPs** (7.8 nm) was evident in the TEM image of **NPF-AuNPs** at pH 3 [Fig. 5(a)], attributable to the greater degrees of protonation of the amino groups on polymer side chains and adsorption on the **AuNP** surfaces. At pH 10.4, the TEM image in Fig. 5(b) reveals less aggregation of **AuNPs**, due to lower content amounts of ammonium groups and resulting decreased adsorption of the polymer onto **AuNP** surfaces. We suspect that the highly protonated amino groups of the alkylated polyamine played a similarly important role as that of the head groups of cetyltrimethylammonium bromide (CTAB) in the selective adsorption onto **AuNP** surfaces [41,46]. Likewise, we attribute the formation of our gold nanostructures to the presence of organic layers of alkylammonium chloride units (in an acidic solution) adsorbed onto the Au surface [47]. The ratio of protonated/deprotonated amino groups at a particular value of pH governed the degree of adsorption through the interactions of these groups with the negatively charged surfaces of the inorganic solids. The driving force is electrostatic force and **NPF** acts as the surfactant of **AuNPs** and keeps the nanoparticles spherical [48]. The size effect of nanoparticles on TEM images is related to the total surface area of **AuNPs**. As a result, the effect of the pH on the adsorption of **NPF** onto **AuNPs** was a very crucial feature influencing the quenching effect of **AuNPs** in the fluorescent **NPF-AuNP** nanocomposite solutions.

### 3.4. Time-resolved fluorescence analysis of *NPF-AuNPs* solutions

To prove the different quenching effects of **AuNPs** on the fluorescent nanocomposite solutions, we surveyed the time-resolved PL emissions of **NPF-AuNP** solutions at different values of pH. Fig. 6 displays the time-resolved fluorescence (TRF) signals of **NPF** and **NPF-AuNP** nanocomposite solutions probed at 421 nm (with excitation at 375 nm). Analysis of the fluorescence decays revealed faster decay of the components in **NPF-AuNPs** solutions relative to

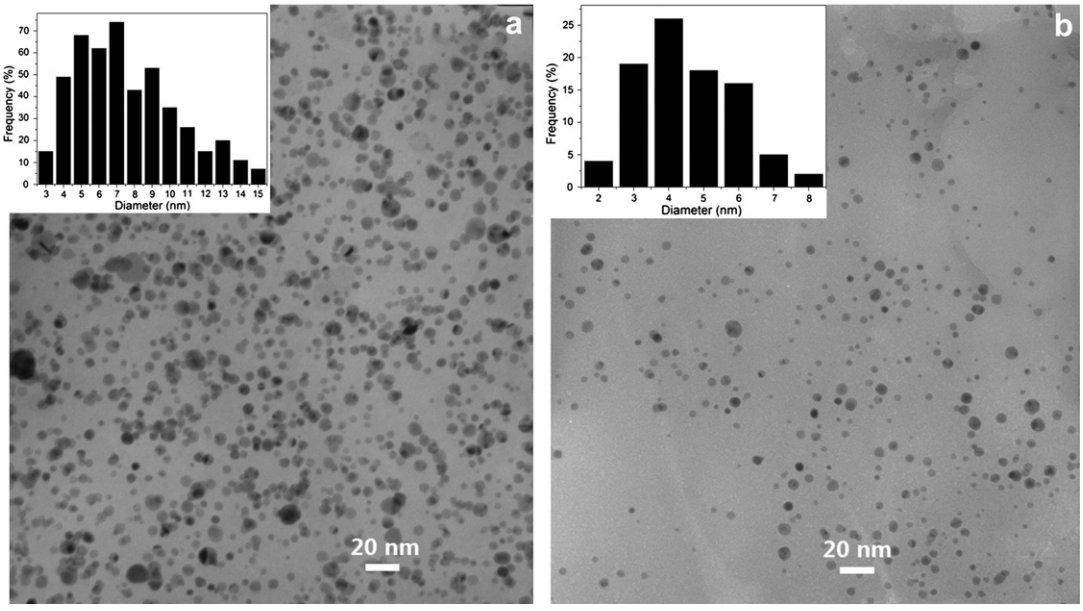


**Fig. 5.** TEM images of **NPF-AuNP** nanocomposites grown from aqueous solutions at (a) pH 3 and (b) pH 10.4.

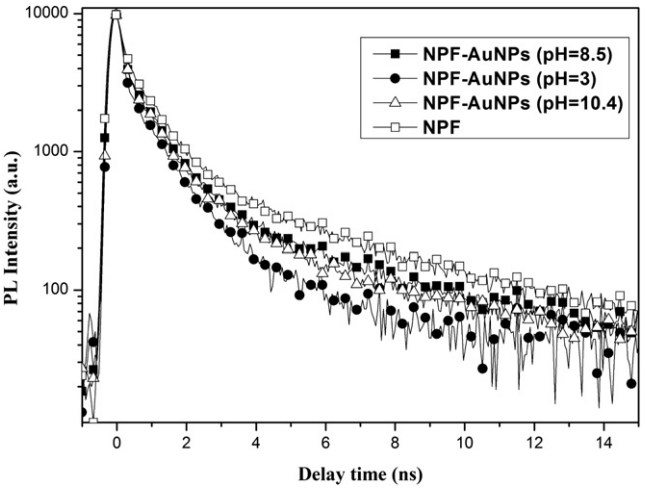


**Fig. 6.** TRF signals of aqueous solutions of **NPF** (empty squares) and **NPF-AuNP** nanocomposites at pH 8.5 (solid squares), pH 3 (solid circles), and pH 10.4 (empty triangles).

those of **NPF**, suggesting that energy transfer occurred from the fluorescent **NPF** to **AuNPs**. Table 1 lists the fluorescence lifetimes obtained through deconvolutions of the instrumental response functions and exponential fittings.

The fluorescence decays of **NPF** at different degrees of protonation and deprotonation are satisfactorily described by biexponential fittings [45], further improving the analytical accuracy. Therefore, we considered the PL decays of **NPF-AuNP** solutions to feature two components: a fast process with a decay time $\tau_1$ and a slow one with a decay time $\tau_2$. Our results suggested that **AuNPs** tended to quench the fluorescence of **NPF** through electron transfer and energy transfer processes in **NPF-AuNP** solutions. A single exponential fitting revealed that the fluorescence lifetime ($\tau_2$) of **NPF** was 3.68 ns, corresponding to the lifetime of the S1 state. When **AuNPs** were introduced into the **NPF** solutions, the ultrafast decay time constant ($\tau_1$) appeared in the biexponential decay fittings. At pH 8.5, $\tau_1$ was equal to 0.46 ns, with a larger content of the faster-decay component ($A_1$ = 65.4%; $A_2$ = 34.5%). More importantly, the presence of the $\tau_1$ decay components in **NPF-AuNP** solutions at different values of pH indicated that the TRF traces consisted of two contributions: one from free **NPF** ($\tau_2$, with lower contribution, due to the lower value of $A_2$) and the other from its composites ($\tau_1$, with higher contribution, due to the higher value of $A_1$). According to the higher contribution of the faster-decay component ($A_1$) in **NPF-AuNP** nanocomposite solutions, the major decay time $\tau_1$ decreased to 0.23 ns at pH 3 and increased to 0.32 ns at pH 10.4, consistent with the degrees of interaction between **NPF** and **AuNPs** that we deduced from the PL and TEM experiments. The quenching of the TRF signals upon the introduction of **AuNPs** to form the nanocomposite solutions implied that the metal surfaces produced a charge-transfer emitting state with **NPF**. Apparently, the interactions between **NPF** and **AuNPs** created another fluorescence quenching pathway in which the presence of ammonium receptors led to effective photoexcited energy transfer from the conjugated main chains of **NPF** to **AuNPs**. The observed fluorescence quenching phenomena of the polymeric surfactants presumably reflected the excitation energy transfer from **NPF** to the metal SPR band of **AuNPs**. Comparing the fluorescence quenching efficiencies of **NPF** by the metal surfaces at different values of pH is a useful tool for constructing adsorption and desorption models for **NPF** on **AuNPs**.

**Table 1**
Fluorescence decay constants for **NPF** in the absence and presence of **AuNPs** at different pH values.

| Polymer or nanocomposite | $A_1$ | $\tau_1$ (ns) | $A_2$ | $\tau_2$ (ns) |
|---|---|---|---|---|
| **NPF**[a] | – | – | 100% | 3.68 |
| **NPF-AuNPs** (pH 8.5)[b] | 65.4% | 0.46 | 34.5% | 2.74 |
| **NPF-AuNPs** (pH 3)[b] | 78.7% | 0.23 | 21.3% | 2.50 |
| **NPF-AuNPs** (pH 10.4)[b] | 75.9% | 0.32 | 24.1% | 2.44 |

[a] The fluorescence decay time constants are calculated by a single exponential fitting.
[b] The fluorescence decay time constants are calculated by a biexponential fitting.

## 4. Conclusions

We have prepared a water-soluble conjugated polymer (**NPF**) presenting side chain ammonium groups for the direct in situ production of **AuNPs**, thereby facilitating the production of **NPF-AuNP** nanocomposites without the need to add any typical reducing agents. We observed greater PL quenching behavior of **NPF** by **AuNPs** and greater aggregation (TEM) of **AuNPs** in the nanocomposite solution at pH 3, relative to those at pH 8.5 and 10.4, as a direct result of the greater degree of protonation of the amino groups on the polymer side chains and, therefore, the greater degree of adsorption onto the **AuNP** surfaces. In contrast to the single exponential fitting of the TRF signals of **NPF** (with a larger lifetime $\tau_2$), the biexponential decay fittings for **NPF-AuNP** nanocomposite solutions revealed two PL decay lifetimes ($\tau_1$ and $\tau_2$). Similar to the results of the PL and TEM experiments, the different TRF decay times $\tau_1$ for **NPF** when quenched by **AuNPs** at different pH values confirmed that stronger interactions existed between **NPF** and **AuNPs** at low pH. The pH-dependent variations in the fluorescent quenching behavior in **NPF-AuNP** nanocomposite solutions might provide a useful tool for constructing adsorption and desorption models for fluorescent water-soluble conjugated polymers on metal nanoparticles; such system might be employed further in forthcoming biotechnological applications.

## References

[1] Chithrani BD, Ghazani AA, Chan WCW. Nano Lett 2006;6:662–8.
[2] Ray PC, Fortner A, Darbha GK. J Phys Chem B 2006;110:20745–8.
[3] Tan YN, Lee JY, Wang DIC. J Am Chem Soc 2010;132:5677–86.
[4] (a) Wang X, Mitchell DRG, Prince K, Atanacio AJ, Caruso RA. Chem Mater 2008; 20:3917–26;
(b) Zhao J, Shan J, Van Assche G, Tenhu H, Van Mele B. Macromolecules 2009; 42:5317–27;
(c) Sardar R, Bjorge NS, Shumaker-Parry JS. Macromolecules 2008;41: 4347–52;
(d) Listak J, Bockstaller MR. Macromolecules 2006;39:5820–5.
[5] (a) Yusa SI, Fukuda K, Yamamoto T, Iwasaki Y, Watanabe A, Akiyoshi K, et al. Langmuir 2007;23:12842–8;
(b) Pérignon N, Marty JD, Mingotaud AF, Dumont M, Rico-Lattes I, Mingotaud C. Macromolecules 2007;40:3034–41;
(c) Ohno K, Koh KM, Tsujii Y, Fukuda T. Macromolecules 2002;35:8989–93;
(d) Li B, Ni C, Li CY. Macromolecules 2007;41:149–55.
[6] (a) Ghosh SK, Pal T. Chem Rev 2007;107:4797–862;
(b) Kim BJ, Fredrickson GH, Kramer EJ. Macromolecules 2008;41:436–47.
[7] Link S, El-Sayed MA. J Phys Chem B 1999;103:4212–7.
[8] Xu XHN, Huang S, Brownlow W, Salaita K, Jeffers RB. J Phys Chem B 2004;108: 15543–51.
[9] (a) Frens G. Colloid Polym Sci 1972;250:736–41;
(b) Kharlampieva E, Slocik JM, Tsukruk T, Naik RR, Tsukruk VV. Chem Mater 2008;20:5822–31;
(c) Jordan R, West N, Ulman A, Chou YM, Nuyken O. Macromolecules 2001;34: 1606–11;
(d) Gupta S, Agrawal M, Uhlmann P, Simon F, Oertel U, Stamm M. Macromolecules 2008;41:8152–8.
[10] (a) Kaewtong C, Jiang G, Ponnapati R, Pulpoka B, Advincula R. Soft Matter 2010;6:5316–9;
(b) Patton D, Locklin J, Meredith M, Xin Y, Advincula R. Chem Mater 2004;16: 5063–70;
(c) Han J, Li L, Guo R. Macromolecules 2010;43:10636–44;
(d) Ginzburg VV, Myers K, Malowinski S, Cieslinski R, Elwell M, Bernius M. Macromolecules 2006;39:3901–6.

[11] (a) Turkevich J, Stevenson PC, Hillier J. Discus Faraday Soc 1951;11:55–75;
(b) Salata OVJ. Nanobiotechnol; 2004;
(c) Meristoudi A, Pispas S. Polymer 2009;50:2743–51;
(d) Ozkaraoglu E, Tunc I, Suzer S. Polymer 2009;50:462–6;
(e) Tanaka M, Fujita R, Nishide H. Polymer 2007;48:5884–8.
[12] (a) Gam-Derouich S, Mahouche-Chergui S, Truong S, Hassen-Chehimi DB, Chehimi MM. Polymer 2011;52:4463–70;
(b) Fuchs AV, Will GD. Polymer 2010;51:2119–24.
[13] (a) Jiang GQ, Baba A, Ikarashi H, Xu RS, Locklin J, Kashif KR, et al. J Phys Chem C 2007;111:18687–94;
(b) Panda B, Chattopadhyay A. J Colloid Interface Sci 2007;316:962–7.
[14] (a) Chia KK, Cohen RE, Rubner MF. Chem Mater 2008;20:6756–63;
(b) Wu C, Szymanski C, McNeill J. Langmuir 2006;22:2956–60;
(c) Zhou Y, Itoh H, Uemura T, Naka K, Chujo Y. Langmuir 2002;18:277–83;
(d) Kumar SS, Kumar CS, Mathyarasu J, Phani KL. Langmuir 2007;23:3401–8.
[15] Kozlovskaya V, Kharlampieva E, Chang S, Muhlbauer R, Tsukruk VV. Chem Mater 2009;21:2158–67.
[16] (a) Fan C, Wang S, Hong JW, Bazan GC, Plaxco KW, Heeger AJP. Natl Acad Sci U S A 2003;100:6297–301;
(b) Costanzo PJ, Beyer FL. Macromolecules 2007;40:3996–4001;
(c) Cole DH, Shull KR, Baldo P, Rehn L. Macromolecules 1999;32:771–9;
(d) Boyer C, Whittaker MR, Luzon M, Davis TP. Macromolecules 2009;42:6917–26.
[17] Phillips RL, Miranda OR, You CC, Rotello VM, Bunz UHF. Angew Chem Int Ed 2008;47:2590–4.
[18] Guan Z, Polavarapu L, Xu QH. Langmuir 2010;26:18020–3.
[19] Xu H, Wu HP, Huang F, Song SP, Li WX, Cao Y, et al. Nucleic Acids Res 2005;33:e83.
[20] Bunz UHF, Rotello VM. Angew Chem Int Ed 2010;49:3268–79.
[21] He F, Tang Y, Wang S, Li Y, Zhu D. J Am Chem Soc 2005;127:12343–6.
[22] Ho HA, Béra-Abérem M, Leclerc M. Chem-Eur J 2005;11:1718–24.
[23] Dulkeith E, Ringler M, Klar TA, Feldmann J, Muñoz Javier A, Parak WJ. Nano Lett 2005;5:585–9.
[24] Lee S, Cha EJ, Park K, Lee SY, Hong JK, Sun IC, et al. Angew Chem Int Ed 2008;47:2804–7.
[25] Fan C, Plaxco KW, Heeger A. J Am Chem Soc 2002;124:5642–3.
[26] Kim TH, Swager TM. Angew Chem Int Ed 2003;42:4803–6.
[27] Qin C, Wu X, Gao B, Tong H, Wang L. Macromolecules 2009;42:5427–9.
[28] Ho HA, Leclerc M. J Am Chem Soc 2004;126:1384–7.
[29] Feng X, Liu L, Wang S, Zhu D. Chem Soc Rev 2010;39:2411–9.
[30] Sudeep PK, Emrick T. Polym Rev 2007;47:155–63.
[31] Shang L, Qin C, Wang T, Wang M, Wang L, Dong S. J Phys Chem C 2007;111:13414–7.
[32] Tang ZY, Kotov NA, Magonov S, Ozturk B. Nat Mater 2003;2:413–8.
[33] Tan C, Atas E, Müller JG, Pinto MR, Kleiman VD, Schanze KS. J Am Chem Soc 2004;126:13685–94.
[34] Huang F, Hou L, Wu H, Wang X, Shen H, Cao W, et al. J Am Chem Soc 2004;126:9845–53.
[35] Liu B, Gaylord BS, Wang S, Bazan GC. J Am Chem Soc 2003;125:6705–14.
[36] Cho JH, Caruso F. Chem Mater 2005;17:4547–53.
[37] Newman JDS, Blanchard GJ. J Nanopart Res 2007;9:861–8.
[38] Zhu HG, Pan ZW, Hagaman EW, Liang CD, Overbury SH, Dai SJ. Colloid Interface Sci 2005;287:360–5.
[39] Davies ML, Burrows HD, Cheng S, Moran MC, Miguel MG, Douglas P. Biomacromolecules 2009;10:2987–97.
[40] Liang TC, Lin HC. J Mater Chem 2009;19:4753–63.
[41] Stork M, Gaylord BS, Heeger AJ, Bazan GC. Adv Mater 2002;14:361–6.
[42] Chen CC, Kuol PL, Cheng YC. Nanotechnology 2009;20:055603–10.
[43] Ishizaka S, Wada T, Kitamura N. Photoch Photobio Sci 2009;8:562–6.
[44] Nerambourg N, Werts MHV, Charlot M, Blanchard-Desce M. Langmuir 2007;23:5563–70.
[45] Chen CC, Hsu CH, Kuo PL. Langmuir 2007;23:6801–6.
[46] Thomas KG, Kamat PV. J Am Chem Soc 2000;122:2655–6.
[47] Ghosh SK, Pal A, Kundu S, Nath S, Pal T. Chem Phys Lett 2004;395:366–72.
[48] (a) Polavarapu L, Qu Xu. Langmuir 2008;24:10608–11;
(b) Chia KK, Cohen RE, Rubner MF. Chem Mater 2008;17:6756–63.